DOI: 10.13009/EUCASS2022-6083
9TH EUROPEAN CONFERENCE FOR AERONAUTICS AND SPACE SCIENCES (EUCASS)

Experimental investigation on fractal/multiscale trippings for passive control of turbulent flow separation

SEPETAUSKAS Vinicius⋆†*, CUVIER Christophe*⋆*, FOUCAUT Jean-Marc*⋆*, VASSILICOS John-Christos*⋆

⋆ *Univ. Lille, CNRS, ONERA, Arts et Métiers Institute of Technology, Centrale Lille, UMR 9014*
LMFL Laboratoire de Mécanique des Fluides de Lille - Kampé de Fériet, F-59000 Lille, France.
Bâtiment M6, Cité Scientifique, Villeneuve d'Ascq, France
vinicius.sepetauskas@centralelille.fr

†Corresponding author

Abstract

An experimental investigation was performed on the control of turbulent flow separation by fractal/multiscale tripping at the LMFL boundary layer (BL) wind-tunnel. The passive devices, with a relative height of k/δ = 0.125, where δ is the BL thickness are located approximately at x = -3.85h upstream from a rounded backward-facing step (BFS) with Re_h = 100,000 and expansion ratio of 1.15, based on the step height h. The recirculation region is studied by 2D2C particle image velocimetry (PIV) in the streamwise-wall-normal $(x-y)$ plane. The downstream region from passive devices, but upstream from step, is studied by 2D3C stereo PIV in the transverse-wall-normal $(z-y)$ plane. The baseline configuration (without devices) is compared to three fractal/multiscale trippings, all having the same properties except for the number of fractal/multiscale iteration. All obstacles have the same frontal area. The recirculation region is smaller for the fractal/multiscale trippings than for the straight baseline configuration, and the size of the recirculation region decreases as the fractal iteration number increases.

1. Introduction

Backward-Facing Step (BFS) is one of the classical geometries used to force flow separation, see Figure 1. Even If the incoming boundary layer is laminar, after the separation point, the flow quickly becomes turbulent.[10] The separated flow curves downward until impinging on the wall, forming the reattachment zone. Despite its simple geometry, a complex flow is generated, and its study and application range from different areas of research such as airfoils at large attack angle, spoiler flows, separation flow behind a vehicle, combustor, mixing chamber, boat, and buildings.[1]

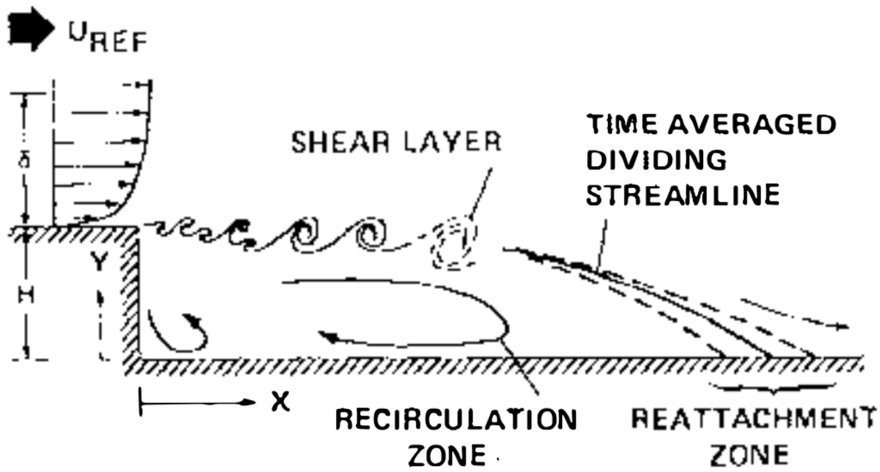

Figure 1: Backward-Facing Step (BFS) sketch. Extracted from Simpson (1989).[10]

Flow Control Devices (FCD) are generally placed upstream from BFS. They can be passive or active. One of the main metrics is the mean flow reattachment location X_R. Several studies show that vortex generators (VG),[5] jets,[3] fences[6] can be used to reduce recirculation region, drag, and noise.

DOI: 10.13009/EUCASS2022-6083

Fractals/multiscale are relatively new, and its application to flow control is still growing. Due to creative designs, infinity configurations can be built and used for different problems. Nedic (2012)[8] used fractal concept for noise reduction. Prigent (2017)[9] used fractal/multiscale trailing edge which end up reducing the vortex shedding energy.
The aim of this experimental investigation is to provoke flow separation and to control it using fractal/multiscale passive FCD. The metric X_R will guide this study regarding how much the reference flow changed compared to the controlled case.

2. Methodology

2.1 The wind tunnel facility

The experiment was conducted in the LMFL boundary layer wind tunnel, see Figure 2. The wind tunnel dimensions are 20 m long, the test section has 1 m height and 2 m width. All sides are made of 10 mm glass, providing full optical access. The free-stream velocity ranges from 1 to 10 m/s (±0.5%). During the experiment, wind speed was 9 m/s. The wind tunnel was in closed-loop configuration with temperature regulation of (20 ± 0.2°C).

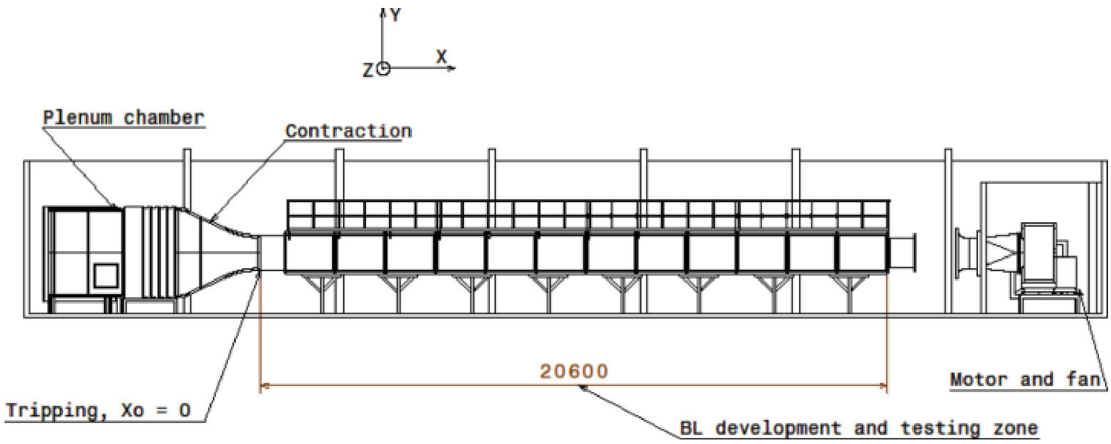

Figure 2: Sketch of the LMFL wind tunnel. Extracted from Cuvier (2017)[2]

2.2 PIV Set-up

The backward facing step (BFS) divides the field into two regions: upstream and downstream, see Figure 3. Both field of views are synchronized, however four cameras responsible for the adverse pressure gradient are at 12 Hz, while the other three are at 192 Hz. This means that every 192/12 = 16 images, they record the same flow.
The upstream region is illuminated by BMI LASER coming from the left, absent in this Figure 3. To avoid wall reflections, the LASER beam is also inclined −5°. The downstream region is illuminated by Quantronix Darwin duo high-speed LASER, its LASER beam can be seen coming from the right in Figure 3. The aim of the high-speed recording of 192 Hz was to capture more than statistics, such as the shedding frequency, and to capture the beginning of the energy spectrum.
It is worth to point out that for high-speed set-up: reference case was recorded 178400 images, while for slow-speed set-up: it was 10500 images. This synchronised experiment were part of another project, and it was done only for the reference case. For the flow control case, only high-speed set-up was used, and fewer images were acquired 19624, as written in Table 1.
The two PIV systems assembly can be seen in Figure 4. The rounded BFS is a semicircle with radius of 130 mm. Flow control devices are placed at x = -500 mm (3.85h) from the step edge, with a step height h = 130 mm. All dimensions in the results' section will be adimensionalised by h, and by the wind tunnel speed of 9 m/s.

2.3 Fractal/multiscale devices

The fractal/multiscale FCD is an addition of sines curves. Each curve has two parameters: amplitude A and wavelength W. Three iterations were built, see Figure 5. At every iteration, A is divided by 2, and W by 4. A 3D rapid prototyping

DOI: 10.13009/EUCASS2022-6083

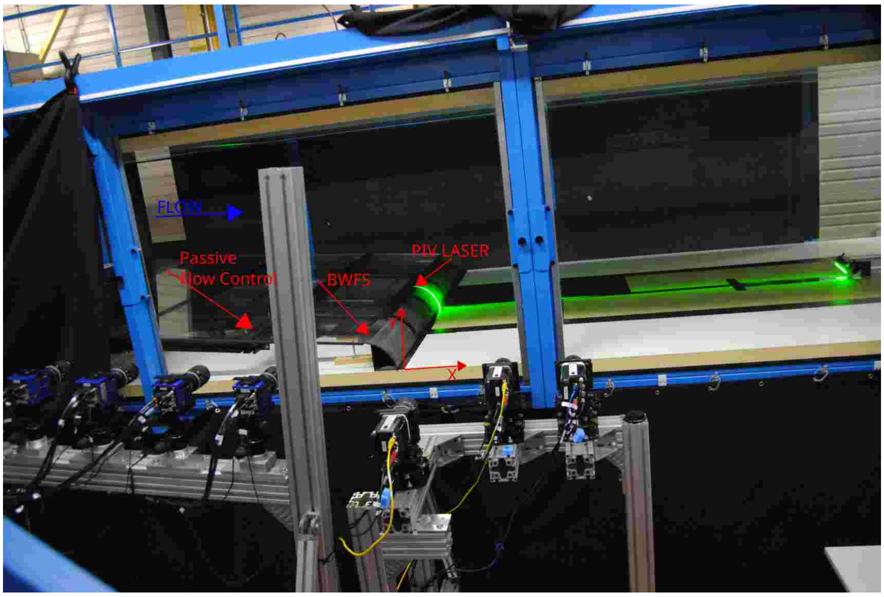

Figure 3: Experiment set-up: Flow direction is from left to right. There are four Low-speed cameras (left) and three High-speed cameras (right). PIV laser is at wind tunnel centerline.

Table 1: PIV recording parameters

Parameters	Low-speed	High-speed
Position	upstream BFS	Downstream BFS
Flow Geometry	Paralell to light sheet	idem
Max. in-plane velocity	$\approx$ 12 m/s	$\approx$ 8 m/s
Camera	Lavision imager sCMOS	Phantom Miro 340
Recording Method	Dual frame/single exposure	idem
Frequency	12 Hz	192 Hz
Recorded images	10,500	19,624
Field of view	$1010^X x213^Y mm^2$ or 2560x2160 px^2	$850^X x100^Y mm^2$ or 2560x860 px^2
Magnification	M $\approx$ -0.066	M $\approx$ -0.086
Overlap	60%	60%
Interrogation window	24x24	24x24
Vector field	988x208	720x86
Illumination 532nm	BMI laser 250mJ/pulse	Quantronix Darwin 25mJ/pulse
Seeding	Glycol-water $d_p \approx 1\mu$m	idem

machine was used to print these fractal curves, the material used is PLA.
The pre-design of the FDC was based on the BL characterization done by Cuvier,[2] together with some advises done by Lin[5] for VG, keeping the height FDC height k smaller than BL thickness for drag concerns, placing the FCD in the range of 6-30k.

DOI: 10.13009/EUCASS2022-6083

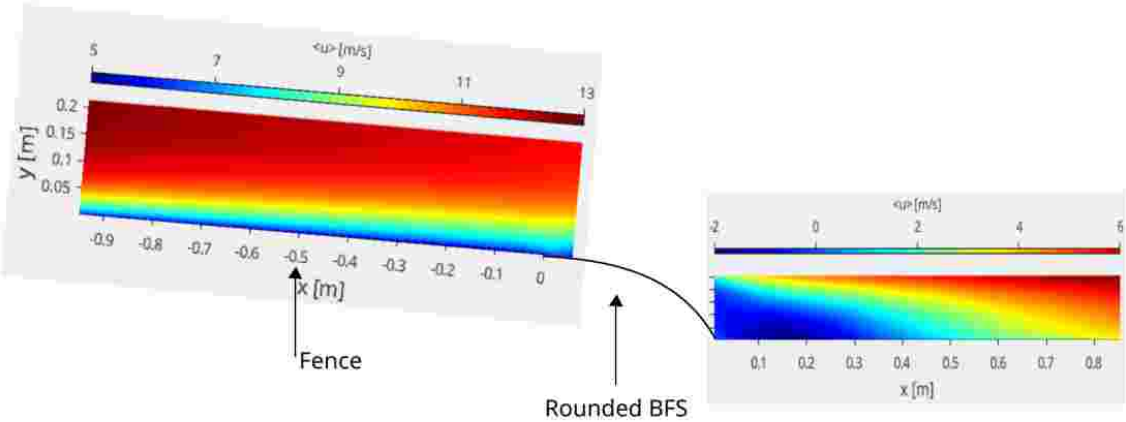

Figure 4: Streamwise mean velocity at upstream (low-speed cameras) and downstream (high-speed cameras) from BFS. Both systems were synchronized only for reference case.

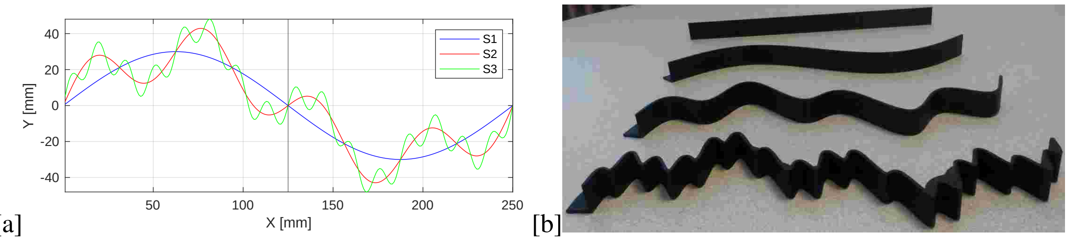

[a] [b]

Figure 5: Fractal-multiscale FCD. a) formed by dividing the amplitude A by 2, and the wavelength W by 4. S1: a simple sine wave A30W250 (blue curve). S2: A30W250 + A15W62.5 (red curve).S3: A30W250 + A15W62.5 + A7.5W15.625 (green curve). b) rapid prototype devices.

3. Results

3.1 Results: Upstream region

A minimum knowledge about the upstream region is paramount for a reasonable estimation of the passive flow control strategy. Unfortunately, due to time constrains and wind tunnel schedule, the creation of the multiscale devices (see Methodology) were done before this first campaign of experiments.Therefore, boundary layer characteristics information were aimed and compared to device height of 20 mm, and x = -3.85h where the passive flow control devices are going to be placed.

This region is not a flat plate with zero pressure gradient (ZPG), but it is an adverse pressure gradient (APG), with ramp angle of $-5°$. The main reason, it is to simulate a more realistic condition where the boundary layer (BL) would be subjected first to a mild APG, followed by a separation (BFS). A summary of flow characteristics is presented in Table 2.

The backward-facing step (BFS) can be considered to have a high Reynolds number based on step height if $Re_h > 36,000$, for expansion ratio $ER < 2$. At this Re_h, mean flow field is nearly independent of Reynolds, and reattachment length is constant.[7] Thus, this campaign at $Re_h = 100,000$ could also be considered as a high Re case.

Now regarding the BL profile over the APG ramp, see Figure 6a, the choice for passive device height of 20 mm [$0.125\delta_{99}$] means that its size is comparable to a micro vortex generators,[5] which are used with an intent to reduce drag while having a flow control effect. The device is about the size of the logarithmic region, see Figure 7b, and strongly interacting with the structures responsible for the second outer peak. The BL evolution against the APG can be followed from farther away upstream x = -7.31h, passing through the FCD location x = -3.85h, and up to the step-edge x = -0.04h without flow separation.

For a first analysis, the choice of log law constants has minor impact on BL profile, and more on drag.[11] As to the latter, it is not our current concern, using the standard constant values of $\kappa = 0.39$ and B = 5, $u_\tau = 0.36$ m/s is a good fit at x = -3.85h, see Figure. 7a. Interesting to note that Cuvier[2] using the same wind tunnel and an elongated ramp (without a step), his friction velocity measured with the help of a high magnification PIV was $u_\tau = 0.36$ at x = -2.17h, and $u_\tau = 0.32$ at x = 2.6h. Showing that for a pre-project planning, the upstream region is not strongly affected when a

DOI: 10.13009/EUCASS2022-6083

Table 2: Flow parameters at APG region, with ramp angle of $-5°$. Reference case, using low-speed PIV set-up

Wind tunnel speed	9 m/s
U_{99} at x = -3.85h	$\approx$ 12 m/s
δ_{99} at x = -3.85h	160 mm
δ^* at x = -3.85h	23 mm
θ at x = -3.85h	16 mm
u_τ at x = -3.85h	0.36 m/s
Re_h	100,000
Re_θ	13,000
Re_τ	4,000
Step height	h = 130 mm
Passive device height	20 mm [$0.125\delta_{99}$]
Expansion ratio	ER $\approx$ 1.15
Wall unit y^+	0.04 mm
First point PIV	$y^+ \approx 29 \approx 1.2$ mm

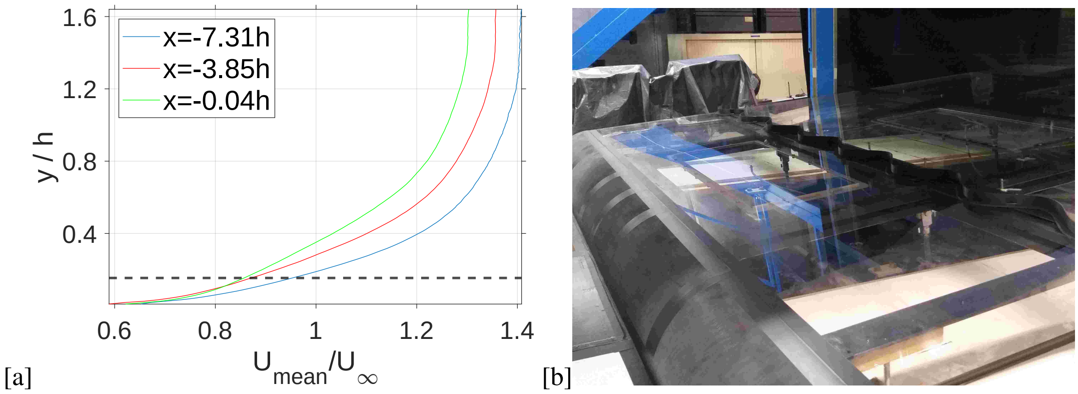

Figure 6: Comparison of BL thickness to the FCD, a) Streamwise mean velocity profiles, the horizontal dashed line at y = 20 mm corresponds to the height of the FCD; b) experimental set-up using FCD S1 case.

rounded BFS is placed at least 3.85h downstream from FCD.
The inner peak $u^+_{rms} = 12 - 15$ is not visible because the first PIV point is at $y^+ = 29$. However, the second peak is visible which is a characteristic of high Re and/or APG region, see Fig 7b.

3.2 Results: Downstream region

In this section, the reference flow can be compared against the controlled cases. The first comparison is the recirculation region size. The streamlines of the mean flow show the recirculation region, see Figure 8. The reattachment position (X_R) can be found by setting streamwise mean velocity to zero $u_{mean} = 0$ which is more convenient when instantaneous recirculation region interface (RRI) are of interest.[12] When average interfaces are of interest, one can use Simpson coef. $\gamma = 0.5$,[10] which means that 50% of the time the flow is upstream. In the reference case, the difference between the two methods is bigger near reattachment region, with $\Delta X_R = 0.1h$ (the same trend happens for all cases). The first PIV measurement point is at 1.2 mm of the wall, and these values presented here are not extrapolated. In this work, the Simpson coef. is the chosen method.
Before the comparison, it is worth to remind that all obstacles (L, S1, S2, S3) have the same frontal area. The reference and straight bar (L) has similar Simpson coef. For each case (S1, S2, S3), three positions (Peak, Middle, Through) are analyzed. All positions had smaller X_R than reference case, see Figure 9. Analyzing individually each multiscale/fractal (S1, S2, S3), the peak has smaller X_R than the middle, and the middle smaller X_R than the through. Another trend is that X_R decreases as the fractal iteration number increases, with exception for through position. One hypothesis made by the author is that multiscale/fractal geometry would force more velocity gradients in different scales and locations. This would exchange more momentum between slow and high speed flow regions. As many other FCD, passive or active, this exchange results in the delay of flow separation or earlier reattachment. In figure 9c, for the through region, the flow reattach earlier than reference. There is a "belly" which makes backflow area bigger as iteration is increased, however the reattachment point is almost at the same position for the three controlled cases. Thus, there are no clear

DOI: 10.13009/EUCASS2022-6083

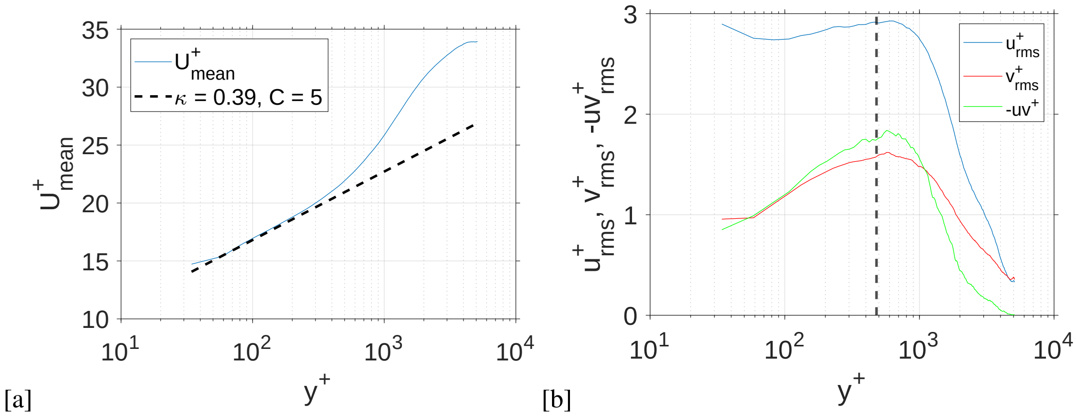

Figure 7: a) streamwise mean velocity profiles in wall units. Inclined dotted-line corresponds to log law. The vertical Dashed line corresponds to $y^+ = 480 = 20$ mm. Streamwise position x = - 3.85h from step-edge. b) mean Reynolds stresses profiles in wall units.

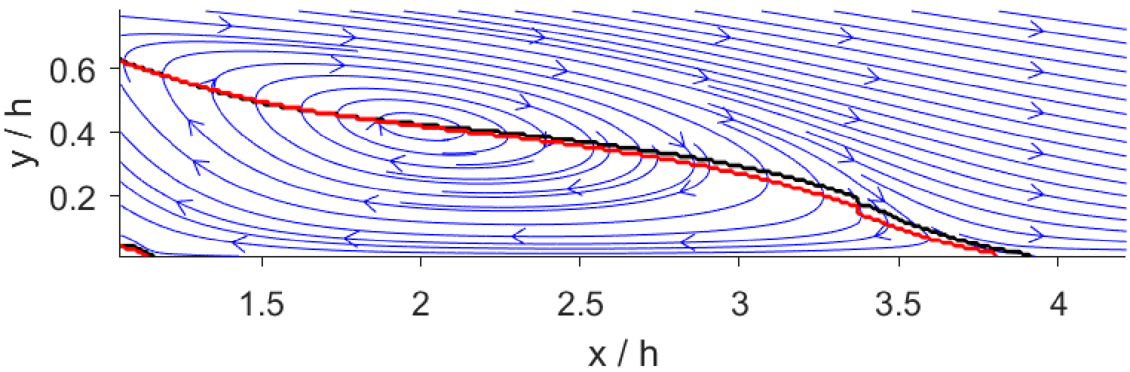

Figure 8: Mean streamlines of the reference separated flow. The black line corresponds to Simpson coef. $\gamma = 0.5$, and the red line to $u_{mean} = 0$. Reference case.

gains for the through region. The three Figures 9a, b, c indicates a strong 3D effects generated by the flow control devices, and it gets stronger with the fractal/multiscale iteration.

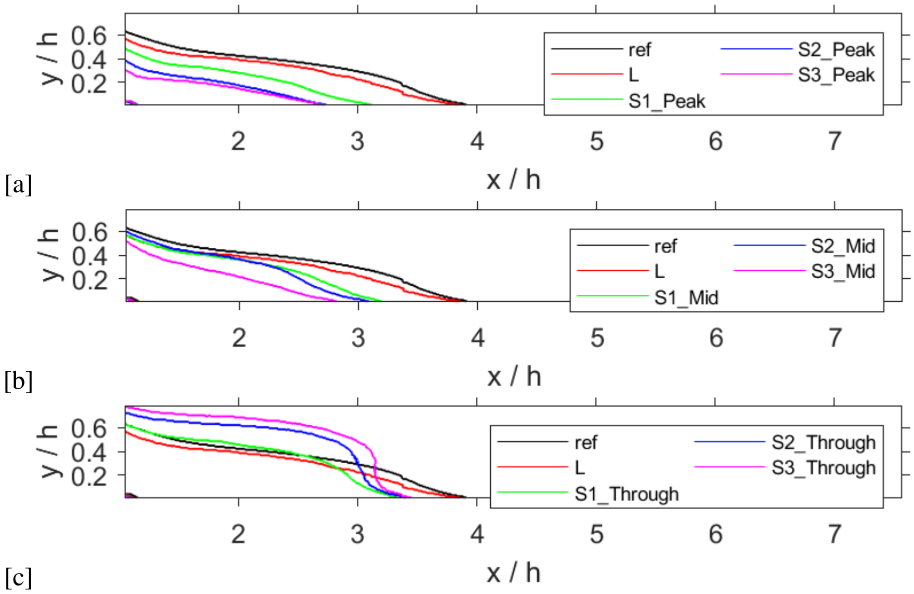

Figure 9: Simpson coef. $\gamma = 0.5$ for a) peak; b) middle; c) through.

DOI: 10.13009/EUCASS2022-6083

Table 3: Reatachment point X_R using Simpsons's coef. $\gamma = 0.5$.

	ref	L	S1	S2	S3
Peak	-	-	3.12h	2.74h	2.71h
Mid	3.92h	3.86h	3.20h	3.09h	2.82h
Through	-	-	3.34h	3.42h	3.46h

The analysis of the statistics of the velocity field shows difference between reference to controlled cases. The streamwise mean velocity in figure 10 indicates a faster velocity recovery further downstream ($x/h > 5$) for peak region, which correlates with a smaller recirculation bubble. In the through region, the X_R, for any case, is smaller than the reference. However the recovery is worse than reference case, which might suggest that X_R location has a weaker effect than recirculation size, once through region does not have a small one, see figure 9c. The mean maximum negative velocity inside the bubble is $0.2U_\infty$, which agrees with the value calculated by DNS.[4]
The increase of the turbulence intensity can be used to delay flow separation or to reduce recirculation bubble. The idea that these flow control devices are increasing the turbulence upstream can not be validated as this experiment is only at downstream region. The streamwise mean Reynolds stress seen in figure 11, has different values but nothing which clearly indicates X_R or bubble reduction. In the middle region, u_{rms} has an increase when compared to reference, which could correlates with bubble size reduction. At the same time, S1, S2, and S3 have similar values regardless of the recirculation reduction as multiscale iteration is increased, see figure 9b. To make it more complex, the u_{rms} decreases at peak region, where clearly has the smaller X_R and bubble size. Thus, streamwise turbulence intensity, at least downstream BFS, can not be correlated to bubble size.

DOI: 10.13009/EUCASS2022-6083

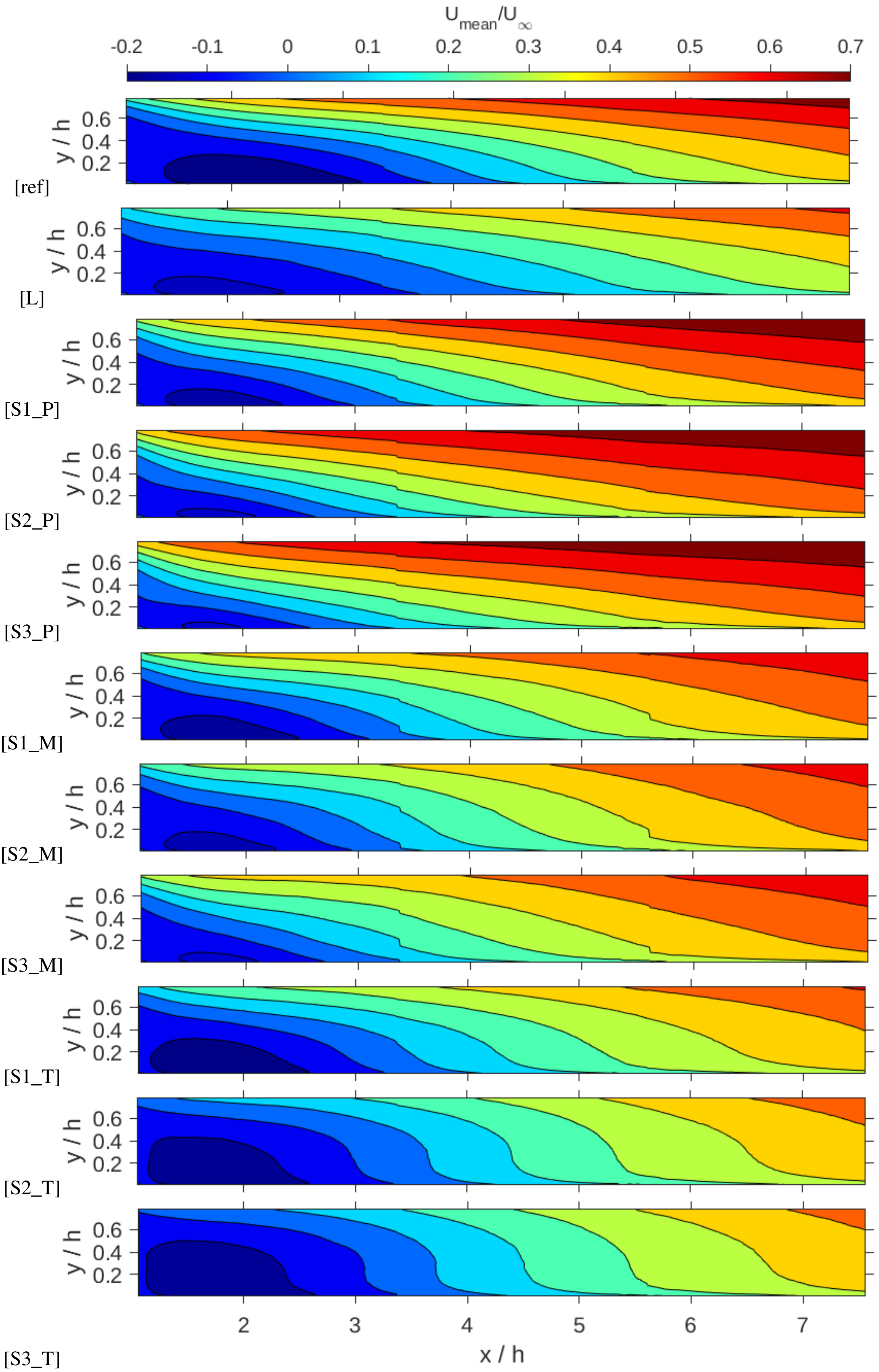

Figure 10: Streamwise mean velocity for peak, middle and through regions.

DOI: 10.13009/EUCASS2022-6083

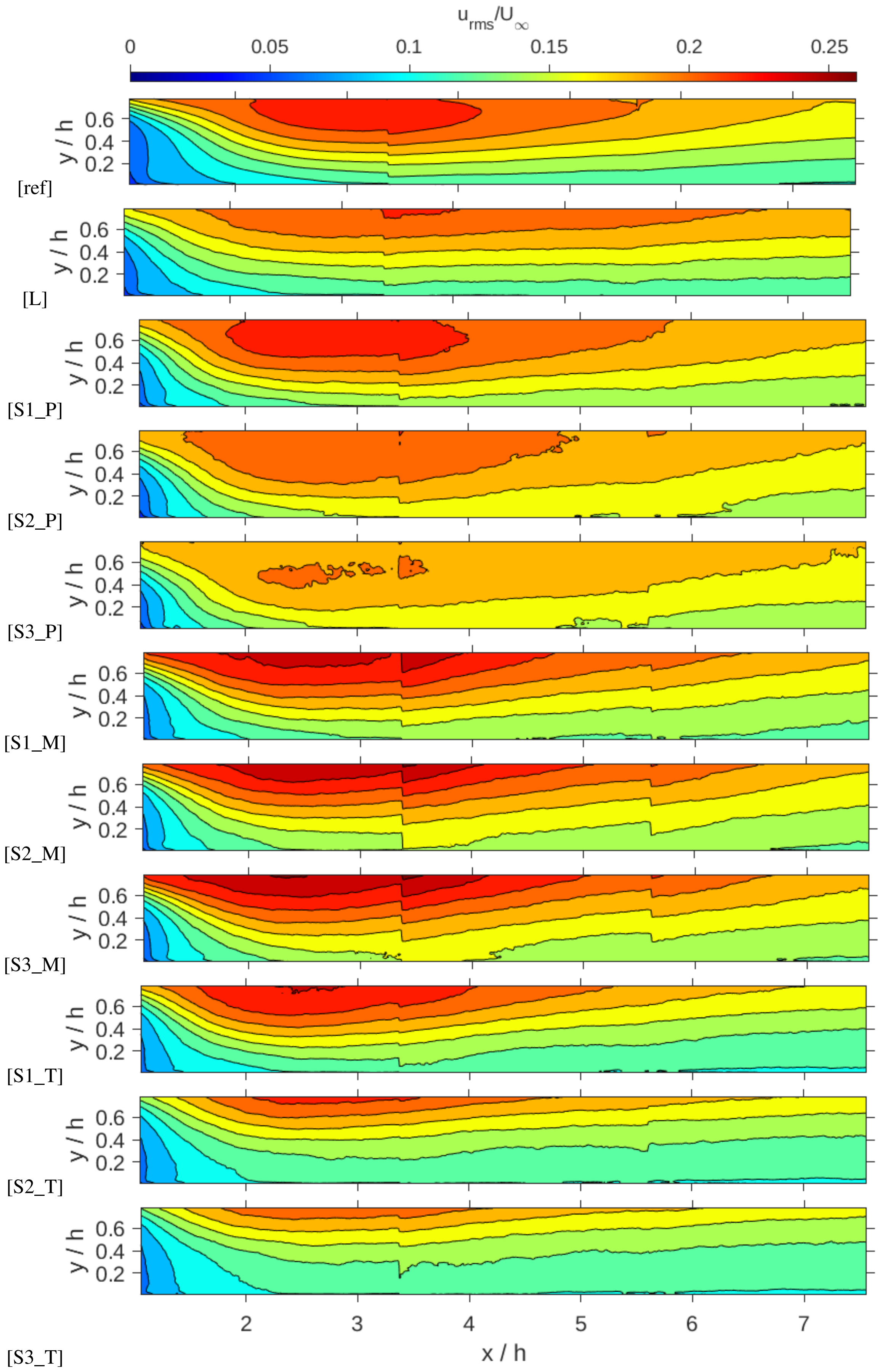

Figure 11: Streamwise mean Reynolds stress for peak, middle and through regions.

DOI: 10.13009/EUCASS2022-6083

4. Stereo-PIV

One of the main objectives, which was to reduce separation region, was accomplished. A Stereo-PIV is important to characterize the transverse flow, once that fractal curves geometry varies along its span. The SPIV set-up uses the same flow conditions as the previous 2D2C-PIV experiment, two Lavision imager sCMOS cameras at 45° degrees angle, 10 000 images at 5 Hz, F# = 5.6, and Innolas LASER of 140 mJ/pulse. There are two SPIV stations, upstream region ST1 = -3.31h and ST2 = -0.04h.

Just before the step-edge, at ST2, the velocity profiles are compared for the middle position. In Figure 12a, the BL profile of fractal/multiscale S1, S2, S3 recovered faster than straight L one, but all controlled cases are far from reference case. As expected, the FCD would produce more turbulence, this can be seen in Figure 12b. However, straight L case, has the same X_R of reference case, indicating that fractal/multiscale need to have another feature which makes them reduce the recirculation region.

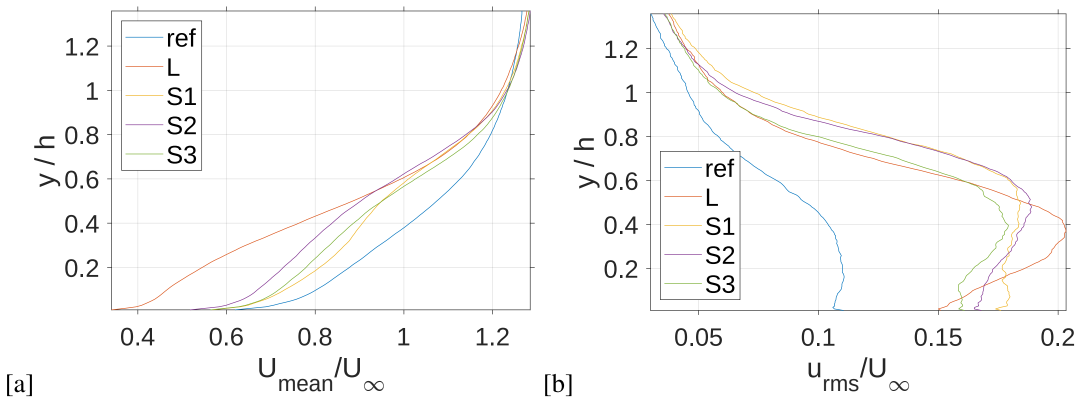

Figure 12: Upstream region at ST2 = -0.04h from step-edge. Wind tunnel centerline. a) Boundary layer profile and b) velocity profile u_{rms}.

Figure 13 shows a large rotating vortex induced by the fractal/multiscale geometry (S1, S2, S3). In the reference and straight L case, the flow has a natural downswash due to the flow descending the rounded BFS. This vortex can be one of the reason why L case did not succeed in reducing the recirculation region.

The fractal/multiscale S1, S2, S3 have differences along spanwise Z, these differences were slightly seen in Figure 13, maybe due to the ST2 be farther away downstream from FDC, the structures generated by the devices might be merged as they are convected by the flow. In order to visualize this history, station ST1 = -3.31h is located near the devices. In Figure 14, SPIV could capture more structures each time that fractal iteration is increased.

DOI: 10.13009/EUCASS2022-6083

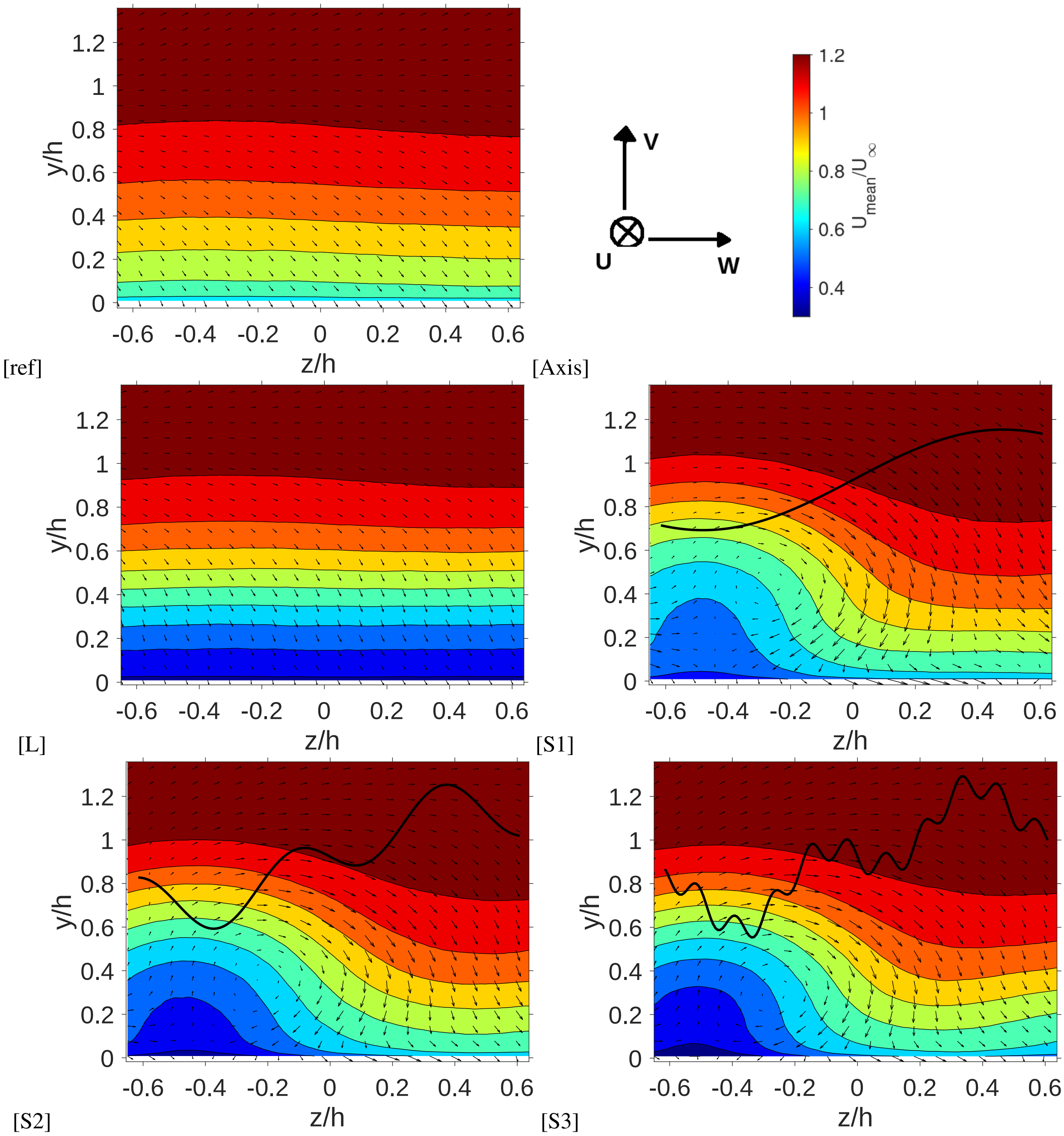

Figure 13: Spanwise and vertical mean velocities represented by the black arrows, streamwise velocity going inside the paper (colorbar). The solid black line represents the fractal/multiscale geometry. Station ST2 = -0.04h from step-edge. Upstream region from BFS.

DOI: 10.13009/EUCASS2022-6083

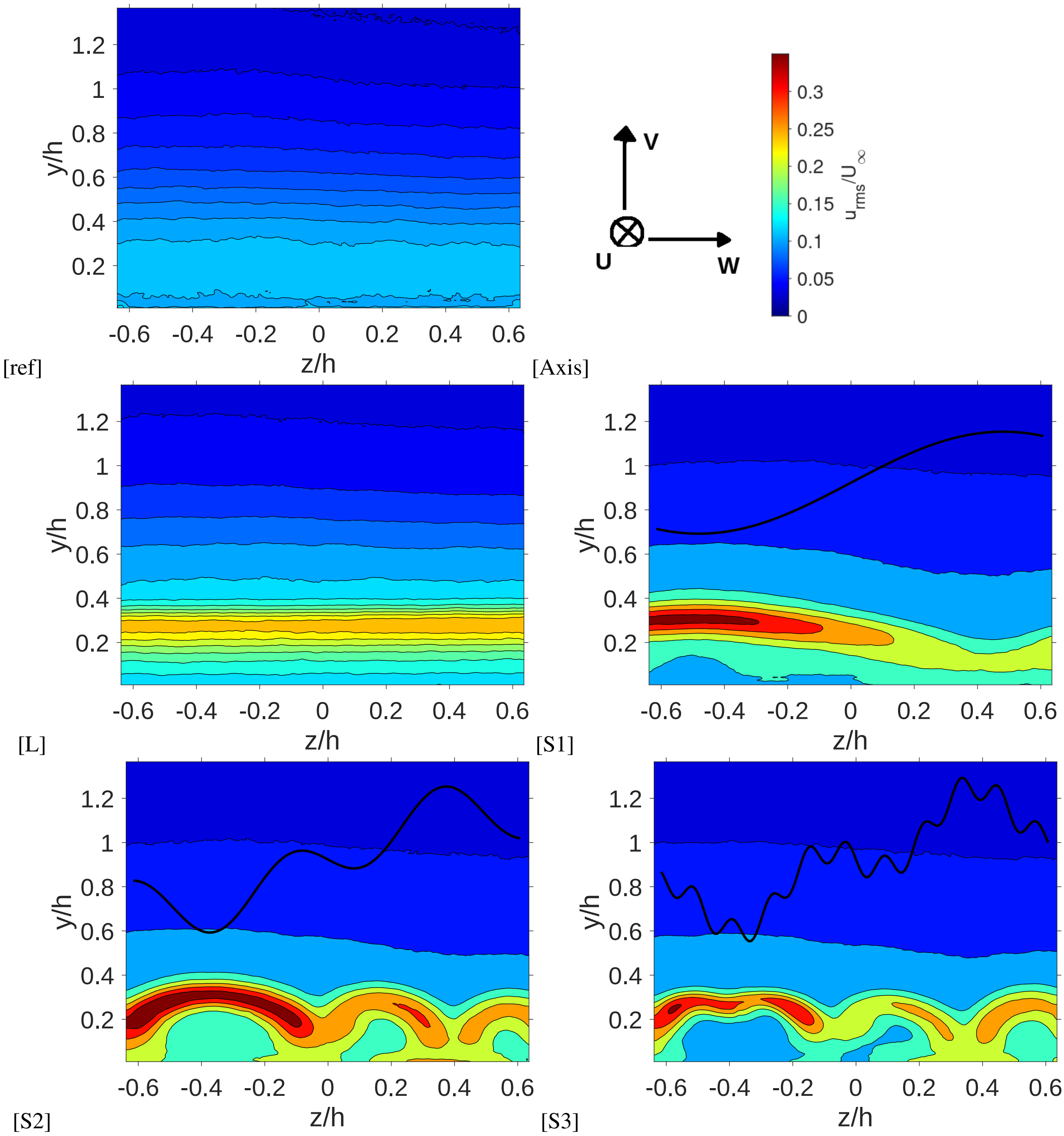

Figure 14: Streamwise mean Reynolds stress. Station ST1 = -3.31h from step-edge. Upstream region from BFS.Solid black line represents the fractal/multiscale geometry.

DOI: 10.13009/EUCASS2022-6083

5. Conclusion

This preliminary fractal/multiscale flow control strategy was investigated experimentally. This new passive device when applied to a rounded backward-facing step (BFS) could affect the flow, reducing the recirculation region. All devices have the same frontal area, but different fractal iteration. Using 2D2C particle image velocimetry (PIV) in the streamwise-wall-normal ($x - y$) plane, the recirculation region is smaller for the fractal/multiscale trippings, and the size of the recirculation region decreases as the fractal iteration number increases. Turbulence intensities alone can not justify the change of X_R location. Thus, a 2D3C particle image velocimetry (PIV) in the spanwise-wall-normal ($z - y$) plane were conducted to investigate 3D effects and upstream condition. It was found that near the fractal/multiscale device is produced more turbulence intensity, and it has a heterogeneous spanwise distribution, with regions with high and low intensity. In another stereo-PIV plane near the step-edge, it could be seen one big mean vortex which suggests that mixing of low and high momentum flow is increased, leading to reduce the bubble size. Results showed the validity of such fractal/multiscale usage for passive flow control approach.

6. Acknowledgments

The work was carried out within the framework of the CNRS Research Foundation on Ground Transport and Mobility, in articulation with the ELSAT2020 project supported by the European Community, the French Ministry of Higher Education and Research, and the Hauts-de-France Regional Council. The authors gratefully acknowledge the support of these institutions.

References

[1] Lin Chen, Keisuke Asai, Taku Nonomura, Guannan Xi, and Tianshu Liu. A review of backward-facing step (bfs) flow mechanisms, heat transfer and control. *Thermal Science and Engineering Progress*, 6:194–216, 2018.

[2] Christophe Cuvier, S Srinath, Michel Stanislas, Jean-Marc Foucaut, Jean-Philippe Laval, CJ Kähler, Rainer Hain, Sven Scharnowski, Andreas Schröder, Reinhard Geisler, et al. Extensive characterisation of a high reynolds number decelerating boundary layer using advanced optical metrology. *Journal of Turbulence*, 18(10):929–972, 2017.

[3] N Gautier and JL Aider. Control of the detached flow behind a backward-facing step by visual feedback'. *arXiv preprint arXiv*, 1306, 2013.

[4] HUNG LE, PARVIZ MOIN, and JOHN KIM. Direct numerical simulation of turbulent flow over a backward-facing step. *Journal of Fluid Mechanics*, 330:349â374, 1997.

[5] John C Lin. Review of research on low-profile vortex generators to control boundary-layer separation. *Progress in Aerospace Sciences*, 38(4-5):389–420, 2002.

[6] Jiun-Jih Miau, KC Lee, MH Chen, and Jung-Hua Chou. Control of separated flow by a two-dimensional oscillating fence. *AIAA journal*, 29(7):1140–1148, 1991.

[7] Pankaj M Nadge and RN Govardhan. High reynolds number flow over a backward-facing step: structure of the mean separation bubble. *Experiments in fluids*, 55(1):1–22, 2014.

[8] Jovan Nedic, Bharathram Ganapathisubramani, John Christos Vassilicos, Jacques Boree, Laurent-Emmanuel Brizzi, and Andreas Spohn. Aeroacoustic performance of fractal spoilers. *Aiaa Journal*, 50(12):2695–2710, 2012.

[9] SL Prigent, ORH Buxton, and PJK Bruce. Coherent structures shed by multiscale cut-in trailing edge serrations on lifting wings. *Physics of Fluids*, 29(7):075107, 2017.

[10] Roger L Simpson. Turbulent boundary-layer separation. *Annual Review of Fluid Mechanics*, 21(1):205–232, 1989.

[11] Alexander J Smits, Beverley J McKeon, and Ivan Marusic. High–reynolds number wall turbulence. *Annual Review of Fluid Mechanics*, 43:353–375, 2011.

[12] Francesco Stella, Nicolas Mazellier, Pierric Joseph, and Azeddine Kourta. Mass entrainment-based model for separating flows. *Physical Review Fluids*, 3(11):114702, 2018.